

## ENTROPY GENERATION ANALYSIS OF NANOFLUID NATURAL CONVECTION IN COAXIAL CYLINDERS SUBJECTED TO MAGNETIC FIELD

by

***Essma BELAHMADI\* and Rachid BESSAIH***

LEAP Laboratory, Department of Mechanical Engineering, Faculty of Sciences Technology,  
University of Frères Mentouri-Constantine 1, Constantine, Algeria

Original scientific paper  
<https://doi.org/10.2298/TSCI171223114B>

*This paper concerns with the effect of a magnetic field on the entropy generation due to natural convection of  $Al_2O_3$ -water nanofluid flow between coaxial cylinders of aspect ratio  $H/D = 2$ . The inner and outer cylinders are maintained at hot and cold temperatures, respectively. The top and bottom walls are thermally insulated. The finite volume method was used to discretize the mathematical equations. The present results are compared with those found in the literature, which reveal a very good agreement. The influence of dimensionless parameters such as Hartmann number, Rayleigh number, solid volume fraction of nanoparticles,  $\phi$ , and inclination angle of magnetic field on streamlines, isotherms contours, local entropy generation, mean Nusselt number, total entropy generation,  $St$ , and Bejan number is discussed. The results show that the local entropy generation are strongly influenced by the application of magnetic field. The increase in heat transfer and entropy generation by adding the nanoparticles to the base fluid depends on the magnetic field strength and direction.*

Key words: *natural convection, entropy generation, nanofluid, magnetic field, coaxial cylinders*

### Introduction

The magnetic field with heat transfer has received considerable attention in recent years because of their wide range of applications in engineering, such as the liquid crystal growth, cooling of nuclear reactors, coating, solidification, float glass production, food processing, microelectronic devices, and solar technology. Improving the thermal characteristics consists in adding small particles to the fluids. Among all the dimensions of particles such as the macro-, micro- and nano-scaled particles *diameter between 1 and 100 nm* attracted more attention because the particles size is close enough to the size of the fluid molecule and the mixture may be more homogeneous.

Mahmoudi *et al.* [1] numerically studied entropy generation due to natural convection in a trapezoidal enclosure using Cu-water nanofluid under magnetic field. They observed that the entropy generation is decreased when the nanoparticles are present, while the magnetic field generally increases the entropy generation amplitude. Salari *et al.* [2] solved the problem of entropy generation induced by natural convection of the Cu-water nanofluid in rectangular cavities with different circular angles and different aspect ratios. The authors showed that the

\* Corresponding author, e-mail: belahmadi.esma@gmail.com

Nusselt number increases with increasing Rayleigh number and solid volume fraction. Mahian *et al.* [3] analytically studied heat transfer of a nanofluid in a vertical annulus under the influence of a magnetic field. The results showed that the use of  $\text{TiO}_2$ -water nanofluid reduces the entropy generation, while a growing Hartmann number increases the entropy generation. Matin and Vaziri [4] analyzed natural convection of a nanofluid in a vertical circular enclosure for different values of Rayleigh number, solid volume fraction of nanoparticles and aspect ratio. They found that the heat transfer characteristic is optimized for physical conditions. Malvandi *et al.* [5] examined numerically the effect of radial magnetic field on forced convection between two concentric horizontal cylinders. The results showed that in the presence of magnetic field, the velocity gradients near the wall grow. Battira and Bessaïh [6] analyzed numerically the effects of axial and radial magnetic fields on steady laminar natural convection in a vertical cylinder with nanofluid. The results indicate that, for low Hartmann number values, the average Nusselt number decreases when the solid volume fraction of nanoparticles is increased; and this decrease is greater if the magnetic field is oriented axially. Afrand *et al.* [7] analyzed natural convection with an induced electric field in a vertical cylindrical annulus filled with liquid potassium. The flow is axisymmetric without a magnetic field, but asymmetrical when the magnetic field is oriented horizontally. Sankar *et al.* [8] analyzed the effect of an axial or radial magnetic field on natural convection in a vertical cylindrical annulus. The authors concluded that the magnetic field suppresses the convection flow and heat transfer rate decreases. Kakarantzas *et al.* [9] carried out the MHD natural convection in a vertical cylinder cavity with sinusoidal upper wall temperature. The results show that the Nusselt number is reduced when the magnetic field is oriented vertically. Rashidi *et al.* [10] performed a numerical study of heat transfer of nanofluid flow in a vertical channel with sinusoidal walls under magnetic field. The results reveal that the average Nusselt number increases by increasing the Grashof number with various values of solid volume fractions.

In the work of Sankar and Do [11], the effect of discrete heating on convective heat transfer in a vertical cylindrical annulus was investigated numerically. Results show that the heat transfer rate increases with the radii ratio and decreases with the aspect ratio. Kakarantzas *et al.* [12] studied natural convection of a liquid metal in a vertical annulus with lateral and volumetric heating. Pourmohamadian *et al.* [13] studied numerically the influence of Brownian motion models on forced convection heat transfer and entropy generation of a nanofluid in a heat source enclosure. The results show that the average Nusselt number increases for all Reynolds numbers. A numerical and analytical study of the disk driven flow in a cylindrical enclosure containing a liquid metal, which is submitted to an axial magnetic field was carried out by Bessaïh *et al.* [14]. The results show that an important damping of heat transfer. Sankar *et al.* [15] studied the effect of a magnetic field on convection driven by buoyancy and surface tension in an annular cylindrical enclosure. The results show that the radial magnetic field is found to be better for suppressing the buoyancy driven flow compared to axial magnetic field. Kakarantzas *et al.* [16] performed direct numerical simulations of MHD liquid metal flow and heat transfer between vertical coaxial cylinders. The results show that the fluid flow increases as the aspect ratio and the annular gap become larger. Gelfgat *et al.* [17] carried out the effect of axial magnetic field on 3-D instability of natural convection in a vertical cylinder filled with a liquid metal. In their paper, the stability diagram was obtained and discussed. Sheikholeslami *et al.* [18] investigated heat and mass transfer of unsteady nanofluid flow between parallel plates. Chamkha *et al.* [19] numerically studied entropy generation and natural convection in C-shaped cavity filled with  $\text{CuO}$ -water nanofluid under to a uniform magnetic field. They observed that the nanoparticles volume fraction enhances the natural convection, but undesir-

ably increases the entropy generation rate. Ismael *et al.* [20] examined numerically entropy generation due to conjugate natural convection-conduction heat transfer in a cavity heated by a triangular solid and filled with a nanofluid CuO-water and saturated porous media and. The authors showed that the addition of nanoparticles increases the entropy generation. A numerical study of nanofluid flow and natural convection heat transfer in a porous media under the influence of electric field using CVFEM was carried out by Sheikholeslami and Seyednezhad [21]. The results show that Nusselt number is an increasing function of Darcy number, supplied voltage and Rayleigh number. Sheikholeslami and Bhatti [22] analyzed numerically forced convection of nanofluid under an uniform magnetic field. The results indicate that Nusselt number enhances with increase of nanofluid volume fraction, Darcy and Reynolds numbers, while it reduces with increase of Lorentz forces. Sheikholeslami [23] performed a numerical simulation of magnetic nanofluid natural convection in a porous curved cavity. The results reveal that heat transfer augmentation augments with rise of Hartmann number and reduces with rise of Darcy and Rayleigh numbers. A numerical investigation of nanofluid free convection under the influence of electric field in a porous enclosure was carried out by Sheikholeslami [24]. The results indicate that Nusselt number is an enhancing function of Coulomb forces and permeability of porous media. Sheikholeslami *et al.* [25] numerically studied nanofluid forced convection heat transfer in existence of magnetic field. They observed that velocity of nanofluid augments with rise of Reynolds number and  $Al_2O_3$  volume fraction but it reduces with increase of Hartmann number.

To the best knowledge of the authors, no such study on heat transfer and entropy generation for MHD natural convection in coaxial cylinders with nanofluid was reported in the literature. In this paper, a 2-D axisymmetric numerical study of laminar natural convection and entropy generation of  $Al_2O_3$ -water nanofluid between vertical coaxial cylinders under the magnetic field was carried out. The effects of magnetic field strength and orientation, concentration of nanoparticles on heat transfer and entropy generation are presented and discussed.

## Problem description and governing equations

### Problem description

The configuration is illustrated in fig. 1. A cylindrical annulus is formed by two concentric cylinders of inner radius,  $R_i$ , and outer radius,  $R_o$ , and subjected to a uniform magnetic field of strength,  $B_0$ , where its orientation forms an angle,  $\gamma$ . The inner and outer walls are maintained at hot,  $T_h$ , and cold temperatures,  $T_c$ , respectively, while the top and bottom walls are adiabatic. The annular cavity of aspect ratio ( $H/D = 2$ , where  $D = R_o - R_i$  is the annular gap and  $H$  the cylinder height) is filled with  $Al_2O_3$ -water nanofluid, which is assumed to have uniform size and in thermal equilibrium. In addition, we assume that the induced magnetic field is negligible, because the magnetic Reynolds number,  $Re_m \ll 1$ .

### Governing equations

By neglecting the dissipation and Joule heating, and introducing the dimen-

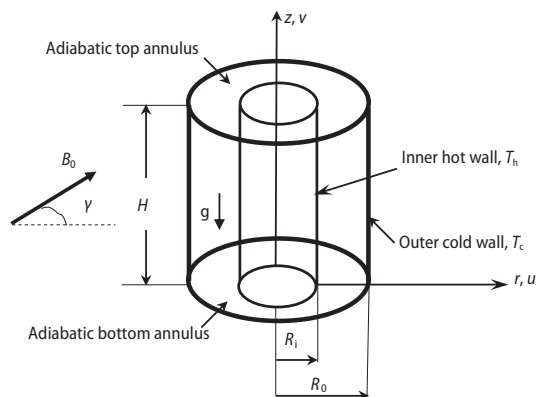


Figure 1. A schematic of the problem and boundary conditions

sional quantities  $D$ ,  $\alpha_{nf}/D$ ,  $(\alpha_{nf}/D)^2$  and  $T_h - T_c$ , for length, velocity, pressure and temperature, respectively, the dimensionless governing equations for steady, 2-D axisymmetric incompressible flow, with constant thermophysical properties, except in buoyancy force (the approximation Boussinesq) are:

$$\frac{1}{R} \frac{\partial}{\partial R} (RU) + \frac{\partial V}{\partial Z} = 0 \quad (1)$$

$$U \frac{\partial U}{\partial R} + V \frac{\partial V}{\partial Z} = -\frac{\partial P}{\partial R} + \frac{\mu_{nf}}{\rho_{nf} \alpha_f} \left[ \frac{1}{R} \frac{\partial}{\partial R} \left( R \frac{\partial U}{\partial R} \right) + \frac{\partial^2 U}{\partial Z^2} \right] + \text{Ha}^2 \text{Pr} \frac{\sigma_{nf}}{\sigma_f} \frac{\rho_f}{\rho_{nf}} (V \sin \gamma \cos \gamma - U \sin^2 \gamma) \quad (2)$$

$$U \frac{\partial V}{\partial R} + V \frac{\partial V}{\partial Z} = -\frac{\partial P}{\partial Z} + \frac{\mu_{nf}}{\rho_{nf} \alpha_f} \left[ \frac{1}{R} \frac{\partial}{\partial R} \left( R \frac{\partial V}{\partial R} \right) + \frac{\partial^2 V}{\partial Z^2} \right] + \text{Ha}^2 \text{Pr} \frac{\sigma_{nf}}{\sigma_f} \frac{\rho_f}{\rho_{nf}} (U \sin \gamma \cos \gamma - V \cos^2 \gamma) + \text{Ra Pr} \Theta \frac{(\rho\beta)_{nf}}{\rho_{nf} \beta_f} \quad (3)$$

$$U \frac{\partial \Theta}{\partial R} + V \frac{\partial \Theta}{\partial Z} = \frac{\alpha_{nf}}{\alpha_f} \left[ \frac{1}{R} \frac{\partial}{\partial R} \left( R \frac{\partial \Theta}{\partial R} \right) + \frac{\partial^2 \Theta}{\partial Z^2} \right] \quad (4)$$

The density, thermal expansion coefficient, thermal diffusivity and heat capacitance of the nanofluid are defined, respectively, as:

$$\rho_{nf} = (1 - \phi) \rho_f + \phi \rho_s \quad (5)$$

$$(\rho\beta)_{nf} = (1 - \phi)(\rho\beta)_f + \phi(\rho\beta)_s \quad (6)$$

$$\alpha_{nf} = \frac{k_{nf}}{(\rho C_p)_{nf}} \quad (7)$$

$$(\rho C_p)_{nf} = (1 - \phi)(\rho C_p)_f + \phi(\rho C_p)_s \quad (8)$$

The viscosity of the nanofluid  $\mu_{nf}$  given by Brinkman [26]:

$$\mu_{nf} = \frac{\mu_f}{(1 - \phi)^{2.5}} \quad (9)$$

Maxwell [27] proposed the thermal conductivity of the nanofluid  $k_{nf}$ :

$$k_{nf} = k_f \left[ \frac{k_s + 2k_f - 2\phi(k_f - k_s)}{k_s + 2k_f + \phi(k_f - k_s)} \right] \quad (10)$$

The electric conductivity of the nanofluid  $\sigma_{nf}$  is calculated [27]:

$$\sigma_{nf} = \sigma_f \left[ 1 + \frac{3(\Delta - 1)\phi}{(\Delta + 2) - (\Delta - 1)\phi} \right], \text{ where } \Delta = \frac{\sigma_s}{\sigma_f} \quad (11)$$

The dimensionless parameters Rayleigh, Prandtl, and Hartmann numbers are defined, respectively:

$$\text{Ra} = \frac{g\beta_f(T_h - T_c)D^3}{\alpha_f\nu_f}, \quad \text{Pr} = \frac{\nu_f}{\alpha_f}, \quad \text{Ha} = B_0D\sqrt{\frac{\sigma_f}{\mu_f}}$$

*Boundary conditions*

The dimensionless boundary conditions for velocity and temperature are:

$$\text{At } Z = 0 \text{ and } R_i \leq R \leq R_o: U = V = 0 \text{ and } \partial\Theta/\partial z = 0 \text{ (bottom annulus)} \quad (12a)$$

$$\text{At } Z = H \text{ and } R_i \leq R \leq R_o: U = V = 0 \text{ and } \partial\Theta/\partial z = 0 \text{ (top annulus)} \quad (12b)$$

$$\text{At } R = R_i \text{ and } 0 \leq Z \leq H: U = V = 0 \text{ and } \Theta = 1 \text{ (inner hot wall)} \quad (12c)$$

$$\text{At } R = R_o \text{ and } 0 \leq Z \leq H: U = V = 0 \text{ and } \Theta = 0 \text{ (outer cold wall)} \quad (12d)$$

*Local and average Nusselt numbers*

The local Nusselt number,  $\text{Nu}(z)$ , is expressed:

$$\text{Nu}(z) = -\frac{k_{\text{nf}}}{k_f} \left( \frac{\partial\Theta}{\partial R} \right)_{R=R_i} \quad (13)$$

The average Nusselt number,  $\overline{\text{Nu}}$ , is calculated:

$$\overline{\text{Nu}} = \int_0^H \text{Nu}(z) dz \quad (14)$$

*Entropy generation*

By using the dimensionless parameter ( $S_{\text{gen}} = s_{\text{gen}}/k_f(T_h - T_c)^2/T_0^2 D^2$ ), the dimensionless local entropy generation written in cylindrical co-ordinates ( $r, z$ ) is:

$$S_{\text{gen}} = \frac{k_{\text{nf}}}{k_f} \left[ \left( \frac{\partial\Theta}{\partial R} \right)^2 + \left( \frac{\partial\Theta}{\partial Z} \right)^2 \right] + \varphi \frac{\mu_{\text{nf}}}{\mu_f} \left\{ 2 \left[ \left( \frac{\partial U}{\partial R} \right)^2 + \left( \frac{U}{R} \right)^2 + \left( \frac{\partial V}{\partial Z} \right)^2 \right] + \left( \frac{\partial V}{\partial R} + \frac{\partial U}{\partial Z} \right)^2 \right\} + \varphi \frac{\sigma_{\text{nf}}}{\sigma_f} \text{Ha}^2 (U \sin \gamma - V \cos \gamma)^2 \quad (15)$$

where

$$\varphi = \frac{\mu_f T_0}{k_f} \left[ \frac{\alpha_f}{D(T_h - T_c)} \right]^2$$

is the irreversibility factor.

The first term of the eq. (15) represents the irreversibility due to heat transfer  $S_{\text{gen,heat}}$ , the second represents the irreversibility due to fluid friction  $S_{\text{gen,friction}}$ , and the third represents the irreversibility due to magnetic field  $S_{\text{gen,magnetic}}$ .

The dimensionless total entropy generation,  $St$ , is calculated:

$$St = \frac{1}{g} \int S_{\text{gen}} d\vartheta \quad (16)$$

where  $\mathcal{V}$  is the total volume of the nanofluid.

Bejan's number is defined as the ratio between irreversibility due to heat transfer and global irreversibility, hence:

$$\text{Be} = \frac{S_{\text{gen,heat}}}{S_{\text{gen,heat}} + S_{\text{gen,friction}} + S_{\text{gen,magnetic}}} \quad (17)$$

### Numerical procedure and validation

The developed code written in FORTRAN language was used to solve the dimensionless eqs. (12)-(15). The second-order accurate central differencing scheme and the SIMPLER [28] were used. The convergence  $U$ ,  $V$ , and  $\theta$  was obtained when the maximum change between two consecutive iterations is less  $10^{-5}$ .

#### Effect of mesh on the numerical solution

Six non-uniform grids are used:  $32 \times 62$ ,  $42 \times 82$ ,  $52 \times 102$ ,  $62 \times 122$ ,  $72 \times 142$ , and  $82 \times 162$  nodes. Table 1 illustrates the variation of  $\overline{\text{Nu}}$  with grid size for  $\text{Al}_2\text{O}_3$ -water nanofluid at  $\text{Ha} = 0$ ,  $\phi = 0.05$ , and  $\text{Ra} = 10^4$ . It is clear that the variation of  $\overline{\text{Nu}}$  remains almost constant from the  $72 \times 142$  and  $82 \times 162$  nodes. Therefore, the grid of  $72 \times 142$  nodes was chosen for all our numerical simulations.

**Table 1. Grid independency results**  
( $\text{Al}_2\text{O}_3$ -water at  $\text{Ha} = 0$ ,  $\phi = 0.05$ , and  $\text{Ra} = 10^4$ )

Grid	$32 \times 62$	$42 \times 82$	$52 \times 102$	$62 \times 122$	$72 \times 142$	$82 \times 162$
$\overline{\text{Nu}}$	7.0336	6.9552	6.945	6.939	6.935	6.933

#### Validation

The first validation with the work of Sankar and Do [11], and Kumar and Kalam [29] at  $R_0/R_1 = 2$  and  $A = H/D = 1$  is shown in fig. 2(a). The second validation with the numerical results of Sankar *et al.* [8] at  $\text{Ra} = 10^5$ ,  $A = 2$ , and  $\text{Ha} = 40$  is illustrated in fig. 2(b). As shown in figs. 2(a) and 2(b), the present results reveal a very good agreement.

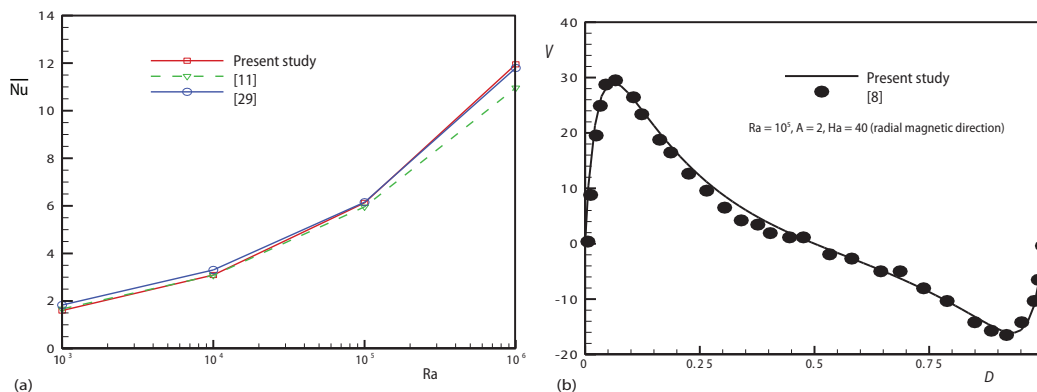


**Figure 2. Validation of the present study with (a) results of Sankar and Do [11], and Kumar and Kalam [29] for the average Nusselt number  $\overline{\text{Nu}}$  at  $R_0/R_1 = 2$  and  $A = H/D = 1$ , (b) results of Sankar *et al.* [8] for the velocity profiles at  $\text{Ra} = 10^5$ ,  $A = 2$ , and  $\text{Ha} = 40$**

### Results and discussion

In this section, we present the effects of magnetic field, inclination angle and nanoparticles fraction on natural convection and entropy generation of  $Al_2O_3$  nanofluid in annular space. All calculations were performed for: solid volume fractions ( $0 \leq \phi \leq 0.1$ ), Rayleigh number ( $10^3 \leq Ra \leq 10^5$ ), Hartmann number ( $0 \leq Ha \leq 100$ ) and inclination angle of magnetic field ( $0^\circ \leq \gamma \leq 90^\circ$ ). The results will be graphically represented in dimensionless form by the streamlines, isotherms contours, local entropy generation, mean Nusselt number, total entropy generation, and Bejan number.

The effect of Hartmann number on streamlines, isotherms contours and local entropy generation at Rayleigh number,  $Ra = 10^5$  and volume fraction of nanoparticles,  $\phi = 0.05$ , is displayed in fig. 3. This figure reveals that the inclination angle of the magnetic field has an effect on the flow field.

When the magnetic field is imposed, it is found that the vortices are no more symmetric. This is due to the presence of magnetic field, which gives rise to the Lorentz force and

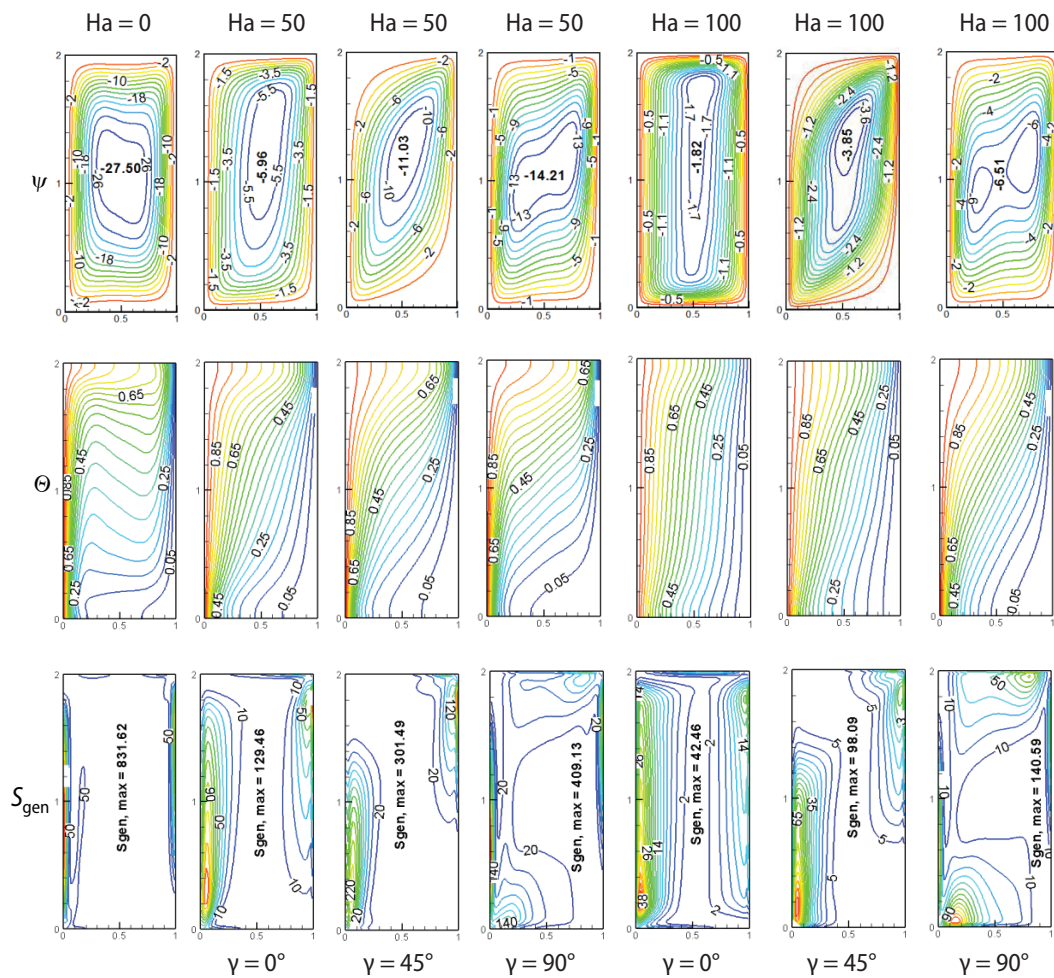


Figure 3. Streamlines,  $\psi$ , isotherms contours,  $\theta$ , and local entropy generation,  $S_{gen}$ , for different Hartman numbers and orientation angles,  $\gamma$ , at  $Ra = 10^5$  and  $\phi = 0.05$

tries to retard the convection. As Hartmann number increases, the circulatory cell is stretched and the flow fills the entire cavity with an increase in the value of maximum stream function from  $-11.03$  at Hartmann number ( $\gamma = 45^\circ$ ) = 50 to  $-3.85$  at Hartmann number ( $\gamma = 45^\circ$ ) = 100. The augmentation of Hartmann number leads to suppress the recirculation formed by the flow into the cavity. At  $Ha = 100$  and  $\gamma = 90^\circ$ , two recirculating cells are formed, which are due to the effect of temperature gradient near the inner and outer side walls, which ensures better fluid flow and contributes to heat transfer augmentation.

The thermal layer near the heated wall is narrower and the isotherms contours become parallel to the hot wall with the increase of Hartmann number, showing the suppression of the convection heat transfer mode dominated by the conduction mode. In addition, the density of the stratified isotherms contours near the hot wall weakens with increasing Hartmann number due to the magnetic field, which is damping the flow. At high Hartmann number values, the isotherms contours that are closer at the left side of the cavity move apart gradually while shifting to the right side. This fact is more pronounced at  $\gamma = 90^\circ$ . As the magnetic field intensity increases, the convection mechanism into the cavity vanishes.

It can be seen that the entropy contours show a symmetrical line and near the side walls, the entropy is higher. The local entropy generation is significant near the heated walls, where the temperature gradient is important. At  $Ha = 100$ , the local entropy generation is maximum near the heated wall. This can occur because after a certain value of Hartmann number. We also note, for  $\gamma = 0^\circ$  and  $45^\circ$ , the entropy generation is higher in the lower region of the left wall.

Figures 4(a)-4(c) depict the variations of the Nusselt number vs. the solid volume fraction for various Hartmann number,  $\gamma$ , and Rayleigh number. The first notable feature of figs. 4(a)-4(c) is that the average Nusselt number increases linearly with increasing the solid volume fraction of nanoparticles. There are two factors that affect the heat transfer while increasing the volume fraction of nanoparticles: The first factor is the increase in the viscosity of nanofluid, which slows its movement, thereby reducing the heat transfer rate; and the second factor is the increase of the thermal conductivity of the nanofluid, which thus improves the heat exchange. The effect of viscosity is less than the effect of conductivity, and therefore the heat transfer rate increases by increasing the solid volume fraction. The variation of the Nusselt number for different Hartmann numbers at  $Ra = 10^4$  and  $\gamma = 90^\circ$  is displayed in fig. 4(a). As expected, for a given value of Rayleigh number, the increase in the Hartmann number dampens the flow in the cylinder by the Lorentz force, which results in a lower heat transfer.

The variation of the Nusselt number for the orientation angle  $\gamma$  and at a fixed  $Ra = 10^4$  and  $Ha = 50$  are displayed in fig. 4(b). It can be ascertained that the averaged heat transfer enhances with magnetic inclination angle, therefore the suppression of heat transfer is more in the case  $\gamma = 0^\circ$  compared to the case  $\gamma = 90^\circ$ . This reveals that at this orientation of the magnetic field ( $\gamma = 90^\circ$ ), the Lorentz force produced allows the fluid circulation in the cylinder without recirculation, which improves the heat transfer.

In fig. 4(c), we show the variation of the Nusselt number for different Rayleigh numbers at  $Ha = 50$  and  $\gamma = 90^\circ$ . The increase in the Nusselt number with the Rayleigh number is due to the fact that an increase in Rayleigh number causes an increase in buoyancy forces. It reveals that the effects of convective heat transfer appear at Rayleigh numbers greater than  $10^4$ , and become dominant when the Rayleigh number takes values greater than  $10^5$ . Selimefendigil and Oztop [30] found that the averaged heat transfer enhances with magnetic inclination angle.

One of the important aspects of our model is to analyze the entropy generation due to the combined effects of magnetic field, natural convection, and solid volume fraction. The combined effect of fluid friction and thermal irreversibility reflects the performance of the ther-

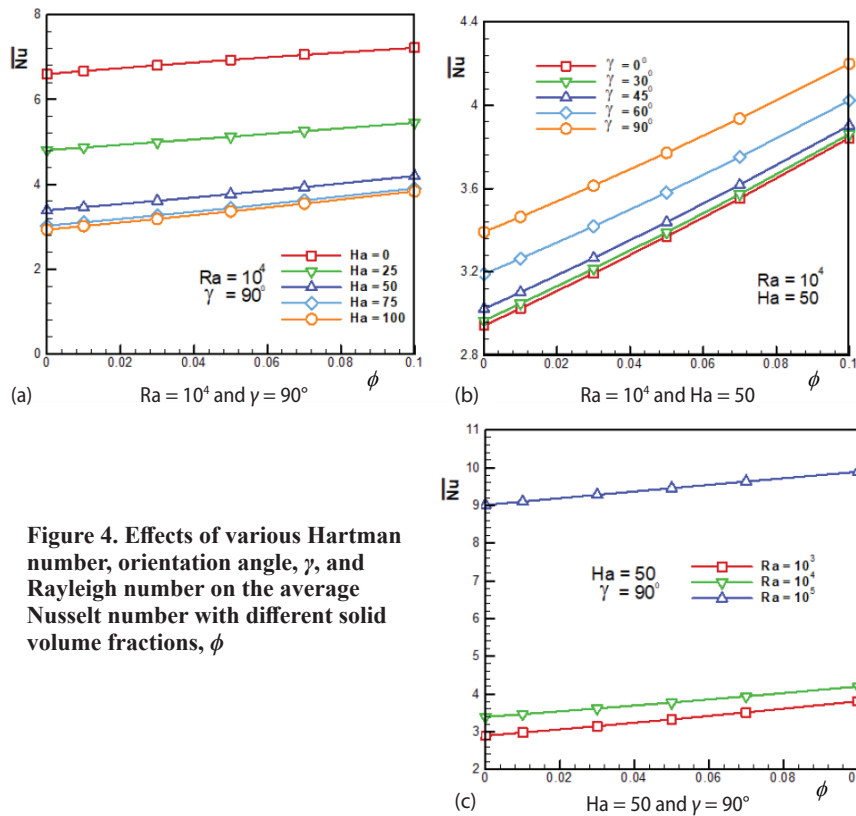


**Figure 4. Effects of various Hartman number, orientation angle,  $\gamma$ , and Rayleigh number on the average Nusselt number with different solid volume fractions,  $\phi$**

mo-fluids characteristics of the channel. There are many practical applications where it is necessary to know the parameter that reduces the entropy generation to improve the thermodynamic efficiency of thermal systems.

Figures 5(a)-5(c) show the effects of solid volume fraction, Hartmann number, inclination angle, and Rayleigh number on the total entropy generation,  $St$ . The obtained results indicate that the increase in the fraction of nanoparticles leads to the increase of the total entropy generation. This can be explained by the increase in the ratios of thermal conductivities and dynamic viscosities of eq. (15). Figure 5(a) shows the variation of the total entropy generation for different Hartmann numbers at  $Ra = 10^4$  and  $\gamma = 90^\circ$ . The increase in the Hartmann number causes a decrease in the entropy generation. This is explained by the attenuation of the flow intensity, which decreases the velocity and temperature gradients. The change in total entropy generation for different  $\gamma$  values at  $Ra = 10^4$  and  $Ha = 50$  is shown in fig. 5(b). At  $Ha = 50$ , the entropy generation increases with increase in the orientation angle of the magnetic field due that to the increase of the flow intensity. This reveals that the entropy generation can be suppressed by applying a radial magnetic field rather than an axial magnetic field. Figure 5(c) shows the variation of the total entropy generation for different Rayleigh numbers at  $Ha = 50$  and  $\gamma = 90^\circ$ . It is found that there is a significant increase of total entropy generation during this convection-dominated regime. It is also found that the maximum value of the entropy generation is obtained when  $Ra = 10^5$ .

Figures 6(a)-6(c) show the effects of the solid volume fraction of nanoparticles, Hartmann number, inclination angle, and Rayleigh number of the magnetic field on the Bejan num-

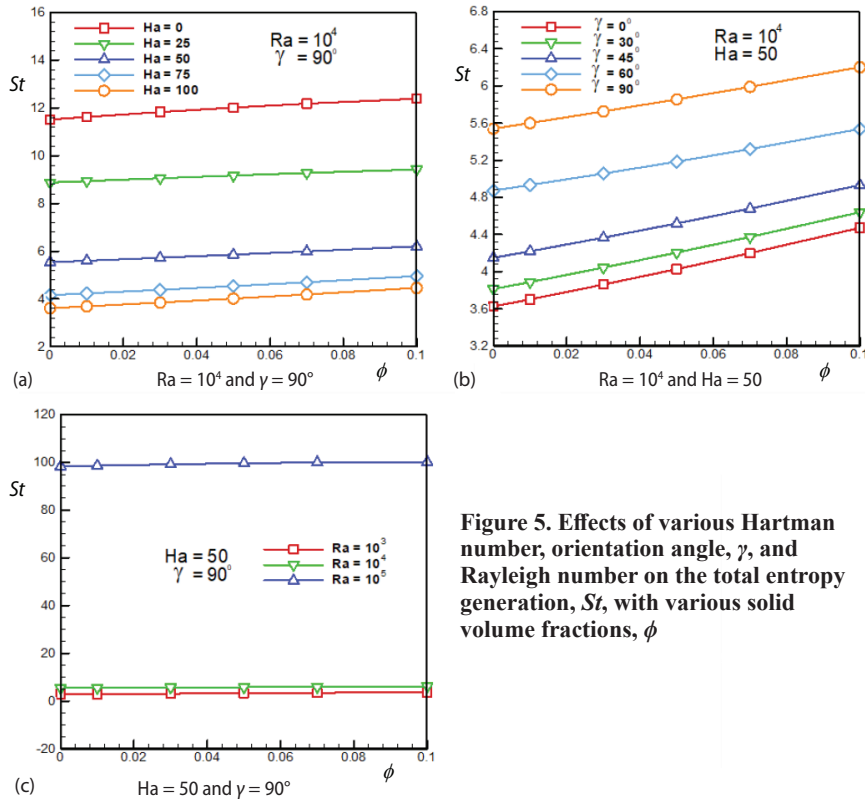


**Figure 5. Effects of various Hartman number, orientation angle,  $\gamma$ , and Rayleigh number on the total entropy generation,  $St$ , with various solid volume fractions,  $\phi$**

ber. For all the configurations studied, Bejan number increases by increasing  $\phi$ , which shows the increase in the irreversibility rate of thermal effects due to the increase of the thermal conductivity by adding nanoparticles to the basic fluid. Figure 6(a) shows the variation of the Bejan number for different Hartmann numbers at  $Ra = 10^4$  and  $\gamma = 90^\circ$ . The Bejan number significantly increases with increasing Hartmann number. It is clear that for  $Ha = 0$ , the Bejan number is less than 0.5, which means that the entropy generation is provided by the fluid friction, contrary to the application of the magnetic field. The variation of the Bejan number for different values of  $\gamma$  at  $Ra = 10^4$  and  $Ha = 50$  is displayed in fig. 6(b). From the figure, it is found that at  $Ha = 50$ , the Bejan number is reduced with increasing inclination angle. It should be noted that for all values of  $\gamma$ , Bejan number is greater than 0.5, indicating the entropy generation is dominated by the temperature gradient. Figure 6(c) shows the variation of the Bejan number for different Rayleigh numbers at  $Ha = 50$  and  $\gamma = 90^\circ$ . It can be seen that increment of Rayleigh number causes contribution of fluid friction to entropy generation. When  $10^3 \leq Ra \leq 10^4$ ,  $Be > 0.5$  indicates that entropy generation is contributed by temperature gradient, while at  $Ra \geq 10^5$ ,  $Be < 0.5$  depicts that entropy generation is contributed by fluid friction.

## Conclusions

In this work, we numerically analyzed the effects of magnetic field strength and orientation, concentration of nanoparticles on heat transfer and entropy generation between vertical coaxial cylinders filled with a nanofluid. The main results are as follows:

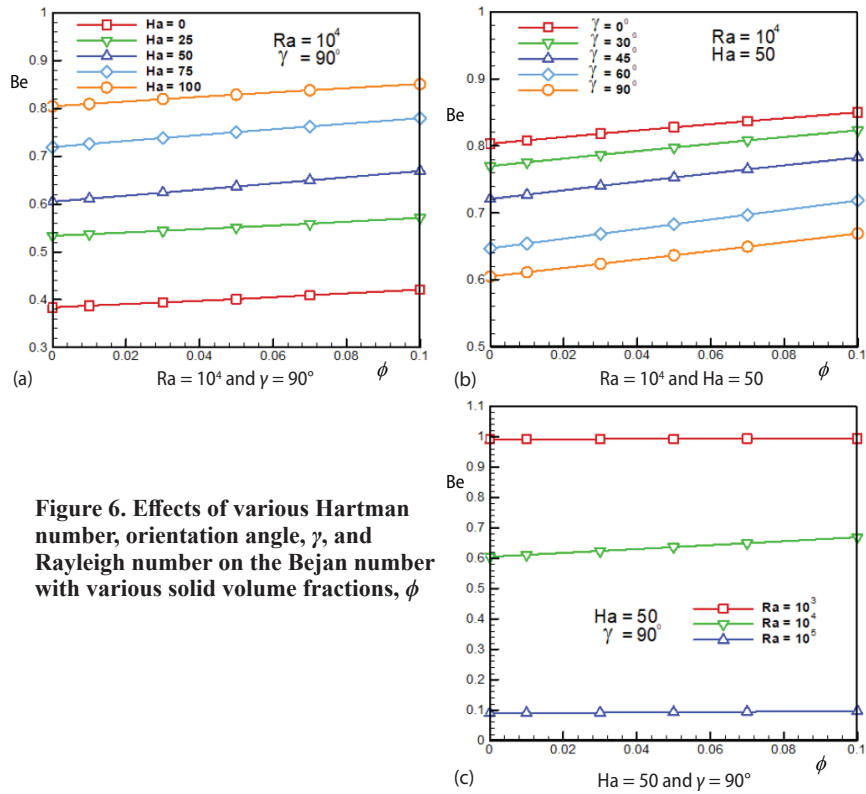


**Figure 6. Effects of various Hartman number, orientation angle,  $\gamma$ , and Rayleigh number on the Bejan number with various solid volume fractions,  $\phi$**

- The intensity and orientation of the magnetic field have an effect on heat transfer and entropy generation.
- Average Nusselt number, total entropy generation and Bejan number increase by increasing the solid volume fraction of nanoparticles.
- Heat transfer and entropy generation decrease and the Bejan number increases by increasing the Hartmann number.
- The heat transfer and entropy generation enhance and the Bejan number decreases with increasing the Rayleigh number and the inclination angle of magnetic field.

### Nomenclature

$B_0$  – magnetic field, [T]  
 $Be$  – Bejan number, [-]  
 $C_p$  – specific heat, [ $Jkg^{-1}K^{-1}$ ]  
 $D$  – annular gap, ( $= R_o - R_i$ ), [m]  
 $g$  – gravitational acceleration, [ $ms^{-2}$ ]  
 $H$  – cylinder height, [m]  
 $Ha$  – Hartmann number, [-]  
 $k$  – thermal conductivity, [ $Wm^{-1}K^{-1}$ ]  
 $\overline{Nu}$  – local Nusselt number, [-]  
 $Nu$  – average Nusselt number, [-]  
 $P$  – dimensionless pressure, [-]  
 $Pr$  – Prandtl number, [-]  
 $R_o$  – outer radius, [m]  
 $R_i$  – inner radius, [m]

$R, Z$  – dimensionless co-ordinates, [-]  
 $Ra$  – Rayleigh number, [-]  
 $St$  – dimensionless total entropy generation, [-]  
 $S_{gen}$  – dimensionless local entropy generation, [-]  
 $s_{gen}$  – local entropy generation, [ $Wm^{-3}K^{-1}$ ]  
 $T$  – temperature, [K]  
 $U, V$  – dimensionless radial and axial velocities, [-]

### Greek Symbols

$\alpha$  – thermal diffusivity, [ $m^2s^{-1}$ ]  
 $\beta$  – thermal expansion coefficient, [ $K^{-1}$ ]  
 $\gamma$  – inclination angle of magnetic field, [ $^\circ$ ]  
 $\phi$  – solid volume fraction

$\phi$	– irreversibility factor	<i>Subscripts</i>	
$\mu$	– dynamic viscosity, [kgm <sup>-1</sup> s <sup>-1</sup> ]	c	– cold
$\nu$	– kinematic viscosity, [m <sup>2</sup> s <sup>-1</sup> ]	h	– hot
$\Theta$	– dimensionless temperature, [-]	f	– fluid (pure water)
$\rho$	– density, [kg m <sup>-3</sup> ]	nf	– nanofluid
$\sigma$	– electrical conductivity, [μScm <sup>-1</sup> ]	s	– nanoparticle
$\psi$	– dimensionless stream function, [-]		

## References

- [1] Mahmoudi, A. H., *et al.*, MHD Natural Convection and Entropy Generation in a Trapezoidal Enclosure Using Cu–water Nanofluid, *Computers and Fluids*, 72 (2013), Feb., pp. 46-62
- [2] Salari, M., *et al.*, Effects of Circular Corners and Aspect-Ratio on Entropy Generation Due to Natural Convection of Nanofluid Flows in Rectangular Cavities, *Thermal Science*, 19 (2015), 5, pp. 1621-1632
- [3] Mahian, O., *et al.*, Irreversibility Analysis of a Vertical Annulus Using TiO<sub>2</sub>/water Nanofluid with MHD Flow Effects, *International Journal Heat and Mass Transfer*, 64 (2013), Sept., pp. 671-679
- [4] Matin, M. H., Vaziri, S., Natural Convection of a Nanofluid Inside a Vertical Circular Enclosure Exposed to a Non-Uniform Heat Flux, *International Communications in Heat and Mass Transfer*, 76 (2016), Aug., pp. 337-347
- [5] Malvandi, A., *et al.*, Effect of Magnetic Fields on Heat Convection Inside a Concentric Annulus Filled with Al<sub>2</sub>O<sub>3</sub>-Water Nanofluid, *Advanced Powder Technology*, 25 (2014), 6, pp. 1817-1824
- [6] Battira, M., Bessaih, R., Radial and Axial Magnetic Fields Effects on Natural Convection in a Nanofluid-Filled Vertical Cylinder, *Journal of Applied Fluid Mechanics*, 9 (2016), 1, pp. 407-418
- [7] Afrand, M., *et al.*, Effect of Induced Electric Field on Magneto-Natural Convection in a Vertical Cylindrical Annulus Filled With Liquid Potassium, *International Journal of Heat and Mass Transfer*, 90 (2015), Nov., pp. 418-426
- [8] Sankar, M., *et al.*, Effect of Magnetic field on Natural Convection in a Vertical Cylindrical Annulus, *International Journal Engineering Science*, 44 (2006), 20, pp. 1556-1570
- [9] Kakarantzas, S. C., *et al.*, Magnetohydrodynamic Natural Convection in a Vertical Cylindrical Cavity with Sinusoidal Upper Wall Temperature, *International Journal of Heat and Mass Transfer*, 52 (2009), 1-2, pp. 250-259
- [10] Rashidi, M. M., *et al.*, Numerical Investigation of Magnetic Field Effect on Mixed Convection Heat Transfer of Nanofluid in a Channel with Sinusoidal Walls, *Journal of Magnetism and Magnetic Materials*, 401 (2016), Mar., pp. 159-168
- [11] Sankar, M., Do, Y., Numerical Simulation of Free Convection Heat Transfer in a Vertical Annular Cavity with Discrete Heating, *International Communications in Heat and Mass Transfer*, 37 (2010), 6, pp. 600-606
- [12] Kakarantzas, S. C., *et al.*, Natural Convection of Liquid Metal in a Vertical Annulus with Lateral and Volumetric Heating in the Presence of a Horizontal Magnetic Field, *International Journal of Heat and Mass Transfer*, 54 (2011), 15-16, pp. 3347-3356
- [13] Pourmohamadian, H., *et al.*, Investigating the Effect of Brownian Motion Models on Heat Transfer and Entropy Generation in Nanofluid Forced Convection, *Thermal Science*, 23 (2019), 2A, pp. 485-496
- [14] Bessaih, R., *et al.*, Hydrodynamics and Heat Transfer in Disk Driven Rotating Flow Under Axial Magnetic Field, *International Journal of Transport Phenomena*, 5 (2003), Dec., pp. 259-278
- [15] Sankar, M., *et al.*, Effect of Magnetic Field on the Buoyancy and Thermocapillary Driven Convection of an Electrically Conducting Fluid in an Annular enclosure, *International Journal of Heat and Fluid Flow*, 32 (2011), 2, pp. 402-412
- [16] Kakarantzas, S. C., *et al.*, MHD Liquid Metal Flow and Heat Transfer Between Vertical Coaxial Cylinders Under Horizontal Magnetic Field, *International Journal of Heat and Fluid Flow*, 65 (2017), Jun., pp. 342-351
- [17] Gelfgat, A. Y., *et al.*, Effect of Axial Magnetic Field on Three-Dimensional Instability of Natural Convection in a Vertical Bridgman Growth Configuration, *Journal of Crystal Growth*, 230 (2001), 1-2, pp. 63-72
- [18] Sheikholeslami, M., *et al.*, MHD Effects on Nanofluid with Energy and Hydrothermal Behavior between Two Collateral Plates: Application of New Semi Analytical Technique, *Thermal Science*, 21 (2017), 5, pp. 2081-2093
- [19] Chamkha, A., *et al.*, Entropy Generation and Natural Convection of CuO-Water Nanofluid in C-Shaped Cavity under Magnetic Field, *Entropy*, 18,50 (2016), 2, 50

- [20] Ismael, M., *et al.*, Conjugate Heat Transfer and Entropy Generation in a Cavity Filled with Nanofluid-Saturated Porous Media and Heated by a Triangular Solid, *Journal of the Taiwan Institute of Chemical Engineers*, 59 (2015), Feb., pp. 1-14
- [21] Sheikholeslami, M., Seyednezhad, M., Simulation of Nanofluid Flow and Natural Convection in a Porous Media under the Influence of electric fields Using CVFEM, *International Journal of Heat and Mass Transfer*, 120 (2018), May, pp. 772-781
- [22] Sheikholeslami, M., Bhatti, M., M., Forced Convection of Nanofluid in Presence of constant Magnetic Field Considering shape effects of Nanoparticles, *International Journal of Heat and Mass Transfer*, 111 (2017), Aug., pp. 1039-1049
- [23] Sheikholeslami, M., Numerical Simulation of Magnetic Nanofluid Natural Convection in Porous Media, *Physics Letters A*, 381 (2017), 5, pp. 494-503
- [24] Sheikholeslami, M., Numerical Investigation of Nanofluid Free Convection Under the Influence of Electric Field in a Porous Enclosure, *Journal of Molecular Liquids*, 249 (2018), Jan., pp. 1212-1221
- [25] Sheikholeslami, M., *et al.*, Numerical Simulation of Nanofluid Forced Convection Heat Transfer Improvement in Existence of Magnetic Field Using Lattice Boltzmann Method, *International Journal of Heat and Mass Transfer*, 108 (2017), B, pp. 1870-1883
- [26] Brinkman, H. C., The Viscosity of Concentrated Suspensions and Solution, *Journal of Chemical Physics*, 20 (1952), 4, pp. 571-581
- [27] Maxwell, J. C., *A Treatise on Electricity and Magnetism*, Vol. 2, Oxford University, Cambridge, UK, 1873, 54
- [28] Patankar, S. V., *Numerical Heat Transfer and Fluid Flow*, McGraw-Hill, New-York, 1980
- [29] Kumar, R., Kalam M. A., Laminar Thermal Convection between Vertical Co-axial Isothermal Cylinders, *International Journal of Heat and Mass Transfer*, 34 (1991), 2, pp. 513-524
- [30] Selimefendigil, F., Oztop, H. F., Conjugate Natural Convection in a Nanofluid Filled Partitioned Horizontal Annulus Formed by Two Isothermal Cylinder Surfaces under Magnetic Field, *International Journal of Heat and Mass Transfer*, 108 (2017), A, pp. 156-171